Development of a Bi-stable Mechanism for Efficiency Optimization of Pneumatic Pressure Boosters

Matthias Schmid, Olivier Reinertz, Katharina Schmitz

RWTH Aachen University
Institute of Fluid Power Drives and Systems (ifas)
Aachen, Germany, matthias.schmid@ifas.rwth-aachen.de

Abstract.

In hydrogen filling stations, pressure boosters are needed to increase the pressure from the level-dependent storage tank to a constant disposal pressure. Pneumatically driven pressure boosters can easily meet the special requirements of explosion protection in such applications. Thus, despite their actually low efficiency, they offer a worthwhile approach. The attractiveness can be further increased by optimizing the efficiency. In state-of-the-art units, a considerable part of the expansion energy in drive chambers is lost due to an unfavorable load over the stroke. By increasing the load at the beginning of the stroke by means of a bi-stable mechanism, the amount of previously unused expansion energy can be stored in it. This energy can be released again in the second half of the stroke. This reduces the pressure requirement at the end of the stroke, allows the air in the drive chamber to expand and thus lowers the air consumption and increases the efficiency. In the scope of this paper, an analytical representation of the pressure booster is shown for an understanding of the thermodynamic processes. On the basis of the simulation model, the load compensation is specified and a concept for the prototype is presented. The concept is based on the negative spring stiffness of a plate during mechanical snap-through. Subsequently, the developed mechanism is integrated into the simulation model and the results and achieved progress are elaborated. Finally, the outstanding measurements and already realized preparations are discussed.

Keywords. gas compression, mechanical snap-through, membrane buckling, spring stiffness, hydrogen

1. INTRODUCTION

For advancing the energy transition an increase in efficiency is also of great interest in pneumatic applications.

Lowering the network pressure is a simple and widely used approach to reduce losses in compressed air systems. However, the pressure demand of a small number of end devices often limits the realizable pressure reduction. To allow a lower system pressure and enhanced efficiency, the operation pressure required by these devices can be generated by

pressure boosters. However, only small boost factors are required for this. The system described in this paper is used for boost factors greater than 2.7.

In the context of the mobility revolution towards sustainable sources of fuel, another use case is emerging. For the use of hydrogen in automotive applications, a high pressure-level of the hydrogen of up to 700 bar is required [1]. Due to the special requirements for explosion protection in hydrogen applications, pneumatically driven systems for pressure boosting are an obvious choice, e.g., in hydrogen filling stations. Thus, pressure boosters offer a worthwhile approach to efficient energy use despite their actual low efficiency. The attractiveness of this device category can be further increased by an efficiency optimization.

In state-of-the-art devices, a significant share of the expansion energy supplied to their drive-chambers is lost due to unfavourable loading of the drive over the stroke. [2] By temporarily storing the previously unused expansion energy in pressure boosters within a bi-stable mechanism, overall efficiency can be increased [3]. A first concept, using a cam loaded by pistons, has already been presented by the co-author. Nevertheless, the presented design is not suitable for industrial application. The basic concept is patent pending. [4] Additionally, the concept of a bi-stabile mechanism has been postulated for usability in vacuum generator. In this paper the principle of a membrane will be used [5].

In the scope of this paper, at first, the examined pressure booster is abstracted for simulation. According to this structure, an analytical representation of the entire system is developed.

At the beginning of the stroke, the load is increased by the mechanical system. The energy thus stored in this mechanism is returned on the second half of the stroke, whereby an approximation to the optimal load profile is achieved. The system is intended to complement pressure boosters already in use, whereby an adaptive design is required to allow operation at varying driving pressures.

The focus of the current investigation is on the dynamic operation. In particular, the change in the stroke frequency caused by the mechanics has a considerable impact on the system´s usability. The aim is to increase efficiency without unreasonably reducing the delivered flow rate. In addition to the numerical simulations of the developed mechanical system, the designed prototype is presented.

The achieved increase in efficiency is shown by means of results from simulative investigation of the reference system compared to the modified device set-up. Finally, in relation to these results, the prototype design and measurement strategy for an experimental validation are discussed.

2. STATE OF THE ART

2.1. Pressure Booster

The principle of the pressure booster works according to Pascal´s Law. Low pressure can be converted into high pressure with the aid of a different area ratio. In the four Chambers shown in Figure 2.1, different thermodynamic processes take place.

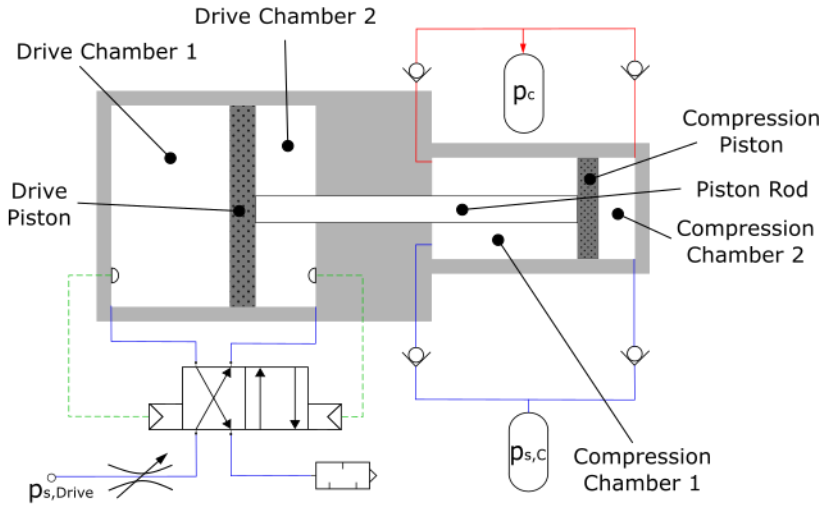

Figure 2.1: Function scheme of the pressure booster

In case of pistons movement to right direction, drive chamber 1 and compression chamber 2 are set as “active chamber”. In opposite direction these are “passive chambers”, as the other chambers are “active”. In the case of the compression chambers, the compression takes place in the first part of the stroke. This increases the resistance against the drive chamber. An isentropic compression is assumed. Once the outlet pressure is reached, a constant driving force is required to push the compressed gas through the corresponding check valve into the high pressure system. A small amount of the compressed gas stays in the dead volume of the chamber at strokes end. Therefore, the gas in the dead volume of the opposite compression chamber is expanded isentropically and supports the movement of the piston.

At the same time, venting to ambient pressure takes place in the directionally related passive drive chamber. The resultant force of the compression chambers and the passive drive chamber lead to a pressure profile of the active drive chamber. The exemplary pressure profile in Figure 2.2 shows an increasing pressure requirement at the end of the stroke. This determines the required pressure level. The aim is to store the pressure potential at the beginning of the stroke and to release it towards the end of the stroke in order to reduce the pressure requirement on the drive side.

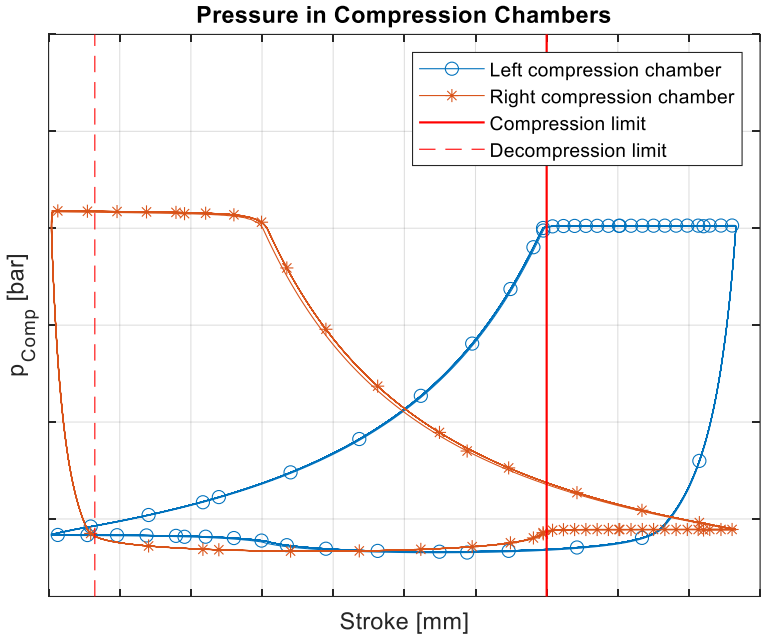

Figure 2.2: Pressure profiles of the compression chambers, 4,5 bar supply pressure, 20 bar compression pressure

In addition to the simulative investigation of the system explained later, an analytical description is presented in the following. This provides an approach to determine the force requirement and serves the general understanding of the process. The equations are based on the equation of motion for the piston. Pressure profiles are implemented in these for the force components corresponding to the piston surfaces. Assumptions are made for the pressure curves. In the case of the active drive chamber, the throttle equation is used for the description. For the complete description of the piston movement during a single stroke, three differential equations are used. The corresponding limits for these differential equations are marked in Figure 2.2. The first stroke section is limited by reaching the complete expansion of the dead volume from the passive compression chamber. This expansion acts supporting to the pistons movement. It is formulated in the fourth term of equation 2.1. At the same stroke section, an isentropic compression process takes place in the active drive chamber. The mathematical formulation is the third term of equation 1. The first term represents the throttle equation for the active drive chamber. For the passive drive chamber, ideal venting is assumed, whereby a constant pressure is added in the second term

$$M_P \cdot \ddot{h} = \frac{-b \cdot p_{S,D}}{\frac{A_{P,D1} \cdot \dot{h}}{C \cdot \rho_0 \cdot R \cdot T} - 1} \cdot A_{P,D1} + p_{D,passiv} \cdot A_{\mathrm{P},D2} + \frac{p_{C\mathrm{omp}} \cdot {h_d}^{\kappa}}{(h_d + h)^{\kappa}} \cdot A_{\mathrm{P},C1}$$

$$- \frac{p_{S,C} \cdot (h_d + h_{max})^{\kappa}}{(h_d + h_{max} - h)^{\kappa}} \cdot A_{\mathrm{P},C2} \qquad (2.1)$$

In the further course until the maximum compression pressure is reached, a constant pressure is established not only in the passive drive chamber but also in the passive compression chamber. The passive compression chamber is filled for the next stroke at the pre-pressure of the process gas. The compression process continues in the active compression chamber.

$$M_P \cdot \ddot{h} = \frac{-b \cdot p_{s,D}}{\frac{A_{P,D1} \cdot \dot{h}}{C \cdot \rho_0 \cdot R \cdot T} - 1} \cdot A_{P,D1} + p_{s,D} \cdot A_{\mathrm{P},D2} + p_{s,C} \cdot A_{\mathrm{P},C1}$$

$$- \frac{p_{s,C} \cdot (h_d + h_{max})^{\kappa}}{(h_d + h_{max} - h)^{\kappa}} \cdot A_{\mathrm{P},C2} \qquad (2.2)$$

In the last section, the maximum compression pressure has already been reached, which means that a constant pressure is now also assumed here in the second term of equation 3.

$$M_P \cdot \ddot{h} = \frac{-b \cdot p_{s,D}}{\frac{A_{P,D1} \cdot \dot{h}}{C \cdot \rho_0 \cdot R \cdot T} - 1} \cdot A_{P,D1} + p_{s,D} \cdot A_{\mathrm{P},D2} + p_{s,C} \cdot A_{\mathrm{P},C1} - p_{C,\max} \cdot A_{\mathrm{P},C2} \qquad (2.3)$$

For performing the experimental investigation, the pressure booster GPLV5 from Maximator is used [6]. The essential technical data are listed in Table 1

Drive stroke diameter	160 mm
Compression stroke diameter	70 mm
Piston rod diameter	20 mm
stroke	94mm
Supply pressure	1 – 10 bar
Maximal compression pressure	60 bar

Table 2.1: Essential technical Data of Maximator GPLV5

A peculiarity of this pressure booster is the mixed form between upstream and downstream throttling, due to the installed valve.

2.2. Bi-stable Mechanism

A bi-stable mechanism is developed for the pressure booster. According to the requirements, it shall store energy at the beginning of the stroke and release it at the end of the stroke. A possible solution to this problem is the use of a buckling shell. In this device energy is stored and returned in the same direction of pistons movement.

Such flexible mechanical structures can be distinguished between stable and unstable behaviour. An example for such structures is a Belleville spring. Figure 2.3 shows the force curve of a Belleville spring with an inner diameter of 80 mm, an outer diameter of 200 mm and a thickness of 0,8 mm. The transition between the two stable end positions leads to an unstable state during the stroke. In the case of the latter, in addition to the bifurcation, there is the snap-through. [7] Hereby the load-deformation curve shows a discontinuity. The area between the reversal points in Figure 2.3 can be understood as negative stiffness. The negative stiffness can be utilised by preloading and stroke limitation in this range [8] [9].

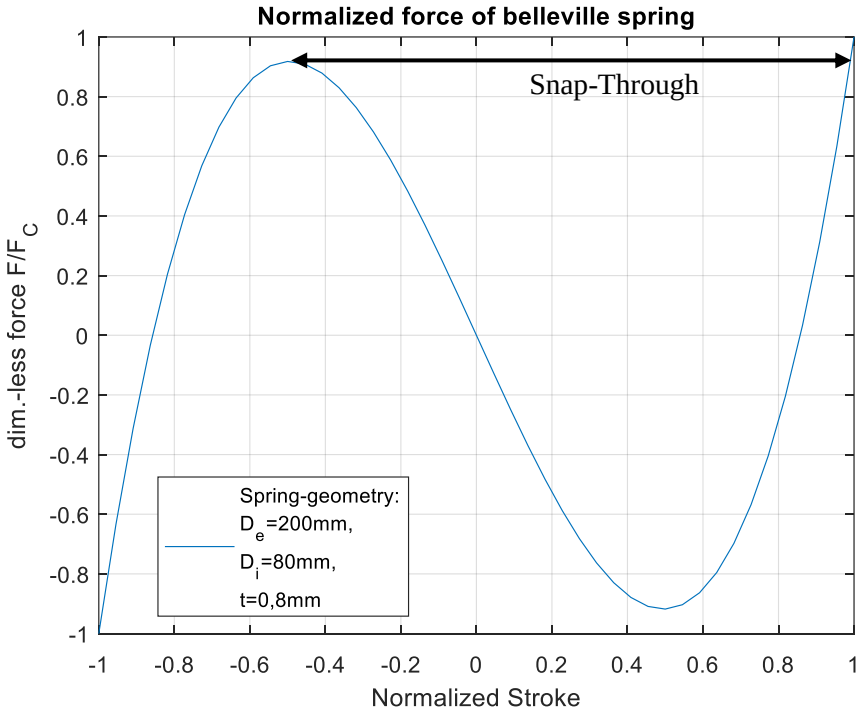

Figure 2.3: Characteristic force curve of a belleville spring according DIN 2092

Based on the simulation, the demand of force in the end positions can be estimated. As already described by Reinertz [3], a negative spring stiffness is required for load compensation.

3. METHODS

In the scope of this paper, the development process of the previously described bi-stable mechanism is explained. For the targeted development, the requirements are defined by means of the reference system. The design of the mechanism is iterated simulatively using FEM. The reference system is also experimentally analysed in preparation for carrying out tests with the new mechanism.

3.1. Determination of the Force Requirement

As stated before, the mechanism shall be used to modify the pressure demand over stroke. Therefore, the optimal force demand is estimated by simulation. The optimum curve is shown in Figure 3.1. In order to ensure functionality for the outward and return movement, the approximated spring stiffness, represented by the diagonal in the diagram, is aimed for.

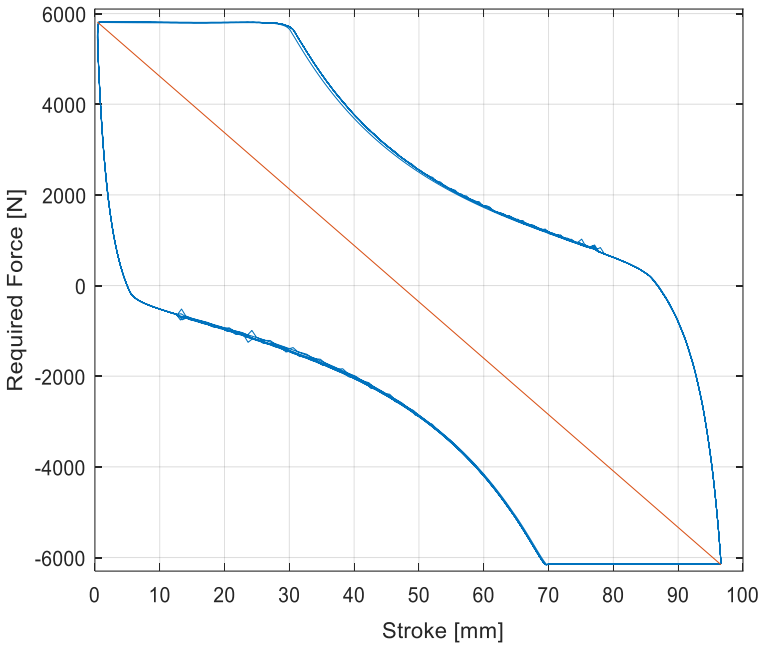

Figure 3.1: Force demand of the mechanics

With the spring described before, a similar force curve can be set. For this purpose, the spring is brought into a preloaded state and the range of movement lies between the force maxima and minima from Figure 3.1.

3.2. Design of Required Mechanism

A promising approach for rectified energy storage and release is mechanical snap-through. This is often realised with membranes First there is a circular plate, that is radially prestressed. This deforms the plate into a spherical shell. During the deformation of the membrane very large radial stresses occur. To circumvent this, the approach of a rectangular sheet is followed. In Figure 3.2 the result of ansys simulation is shown. Essential point of development is the critical stress. The colour steps refer to yield strength of steel 1.4410 and titan Grade 26. Thereof areas of plastic deformation can be identified.

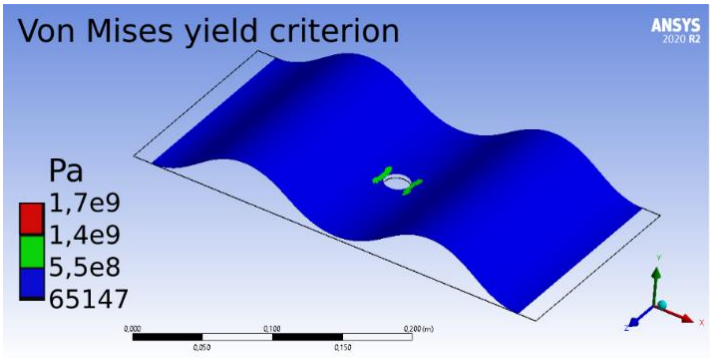

Figure 3.2: Large deformation simulation of rectangular sheet (thickness 0,4 mm) by means of Ansys

This sheet is firmly clamped on the two short sides. Simulatively, the geometry is optimised under the conditions of large deformations in transient dynamics. The main goal here is the reduction of stress. A first approach is to change the cross-section area and thereby the area moment of inertia. A balance between the reduction of the area moment of inertia and the resulting change in stiffness must be ensured. Increasing the size of the spring is another approach.

3.3. Experimental Setup

Two modifications to the commercial hardware are essential for the experimental setup. On the one hand, a way to attach the spring and on the other hand the conversion to upstream throttling. To insert the spring into the power flow, the piston rod on the existing pressure booster is extended on one side and guided outwards through the housing. The piston rod is extended on the drive side to influence the compression ratio as little as possible. The spring can be centrally fixed on the extended piston rod, while at the same time easy access to the pre-stressing of the spring is ensured. The attachment device with pressure booster is shown in figure 3.3.

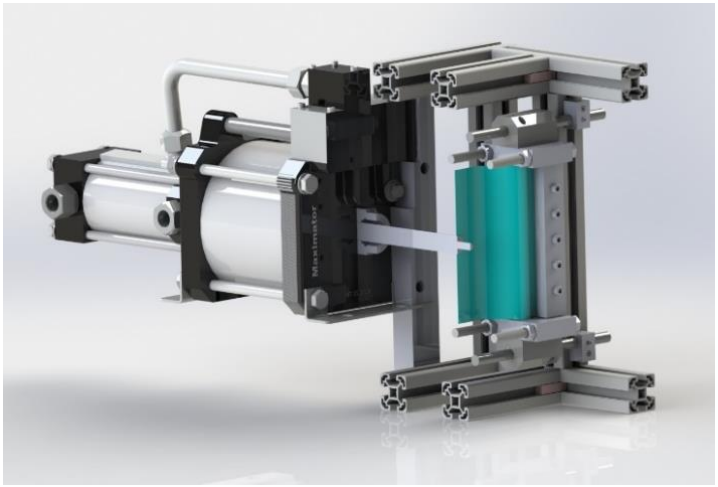

Figure 3.3: Attachment device on pressure booster

Apart from the higher efficiency of an upstream throttling itself, this is mandatory for the mechanics. The upstream throttling ensures that at the end of the stroke the required force from the mechanism takes place and that the drive pressure required up to that point actually decreases. So the drive chamber is not filled to the supply pressure again the drive chamber, as is also the case with the switchover at the end of the stroke. A closer look at the cross-sections of the exhaust air ducts reveals constrictions in the cross-section. Within the scope of the modification these cross-sections were enlarged in order to minimise the effect of downstream throttling.

4. RESULTS

In this section the simulation and measurement results are presented. First, the pressure profiles of the simulated devices are explained. Here, the results of later explanations are already anticipated in order to illustrate the necessity and the effect. Then the spring is described in more detail. The focus is on the geometry for the intended measurements. Finally, the measurement results from the standard device and after modification for upstream throttling are discussed.

4.1. Pressure Profile

The implementation of the negative stiffness in the existing simulation model shows a decreasing pressure demand at the end of the stroke. In contrast, the pressure required at the beginning of the stroke increases to the level of the supply pressure in the modified variant in figure 4.1. The approximately 10% lower pressure demand at the end position of the piston shows the desired effect.

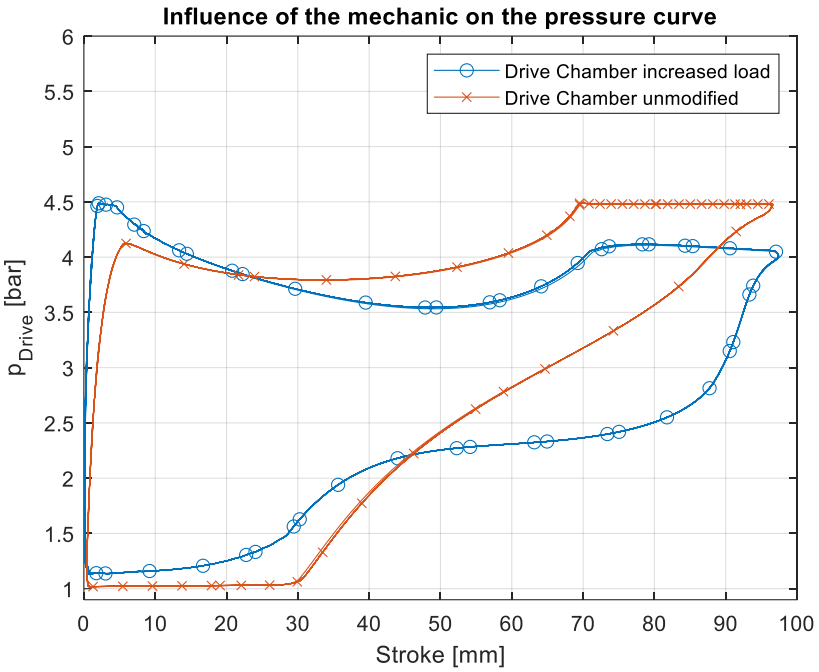

Figure 4.1: Simulated pressure profile of drive chambers with/ without developed mechanism; 4,5 bar supply pressure, 20 bar compression pressure

The additional force from the mechanism prevents the load-free high acceleration of the piston at the stroke begin. This effect can be seen in the time course of the stroke compared to the load-free variant, shown in Figure 4.2. At the same time, the movement of the piston of the unmodified system slows down considerably in the subsequent compression and delivery phase of the gas. The implemented mechanism has a supporting effect in this section, resulting in an approximately constant speed. Moreover, this modification also provides an increase in performance in addition to the energy savings shown above. Thy cycle time of the modified version is considerably shorter, which leads to an increase in delivered flow.

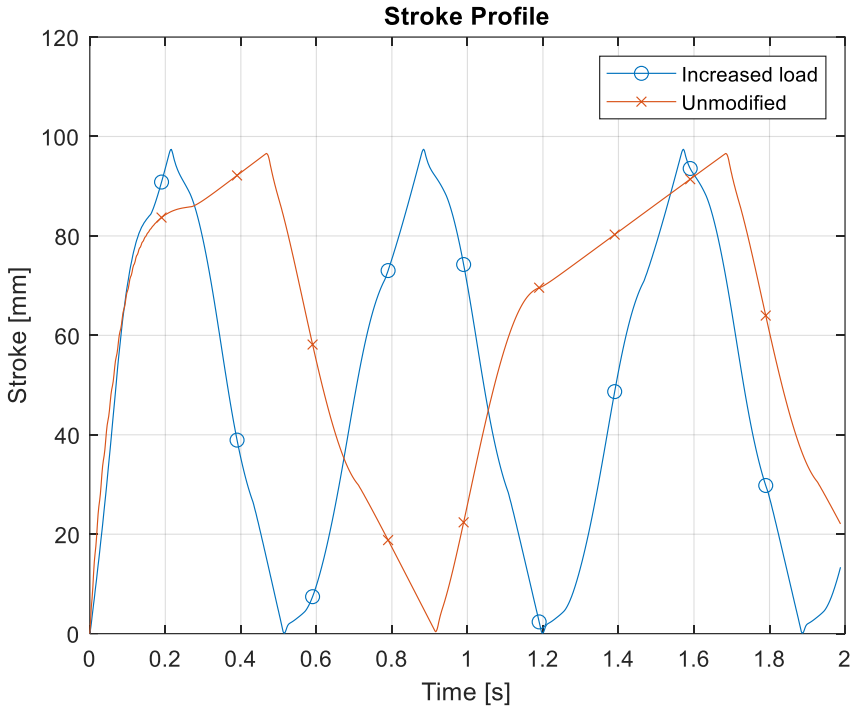

Figure 4.2: Simulated stroke curve with/without developed mechanism; 4,5 bar supply pressure, 20 bar compression pressure

4.2. FEM of the Spring in Snap-Through

Within the scope of the simulation of transient structural mechanics, the stress distributions and the strain behaviour are assessed. The starting point for the simulation procedure is a rectangular sheet. Titanium grade 5 alloy is assigned as the material. The described pre-stress is achieved by pushing the two short flanks together. Meanwhile, the centre of the sheet lifts. This boundary condition is implemented as a displacement in the simulation. Here, a non-linearity between the displacement of the flanks and the displacement of the centre need to be considered. Otherwise, undesired deformations already occur here. As a result, the stress level can exceed the yield strength or even the tensile strength. Compared to the linear displacement of the flanks, a degressive displacement must be applied to the centre. To keep the strains bearable at the large deformations, a sheet thickness between 0.2 mm and 0.3 mm is targeted. Due to the thin geometry, a one-element meshing over the thickness results for the meshing model as a solid shell. The force curve is of decisive importance. This is shown in Figure 4.3.

There is an asymmetry depending on the stroke direction. The cause is the buckling of the sheet. The buckling itself is already asymmetrical depending on the stroke direction. This shifts the zero crossing.

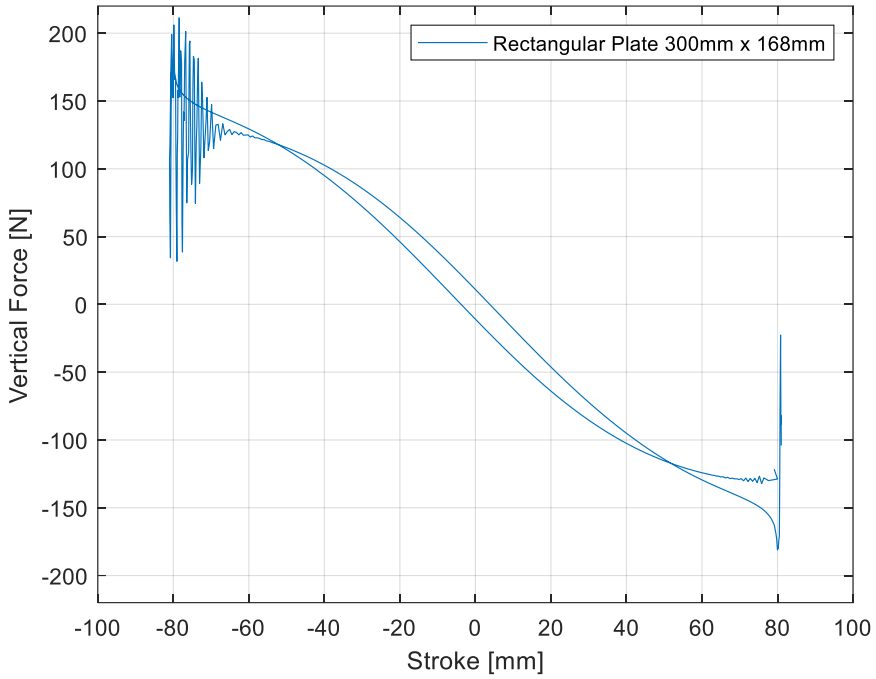

Figure 4.3: Simulated force curve of the spring in the preloaded state

Due to the poor availability of the chosen material, an investigation of available alternatives is necessary. The ferritic stainless steel 1.4410 shows a similar force curve in a first rudimentary simulation. In combination with the variation of the geometric dimensions, a suitable solution can be developed from this. However the maximum force is about 150 N, depends on available material, an individual count of springs are required.

4.3. Measurement Results

Figure 4.4 shows the pressure curve in a drive chamber in comparison between the original condition of the device and the modified version with upstream throttling. There is an improvement in the venting of the drive chamber. At the same time, this reduces the pressure requirement in the first stroke section in the active process. This results in a higher proportion of usable expansion energy. At the same time, the stroke frequency increases. This offers the approach of an additional external upstream throttling to further strengthen the previously mentioned effect.

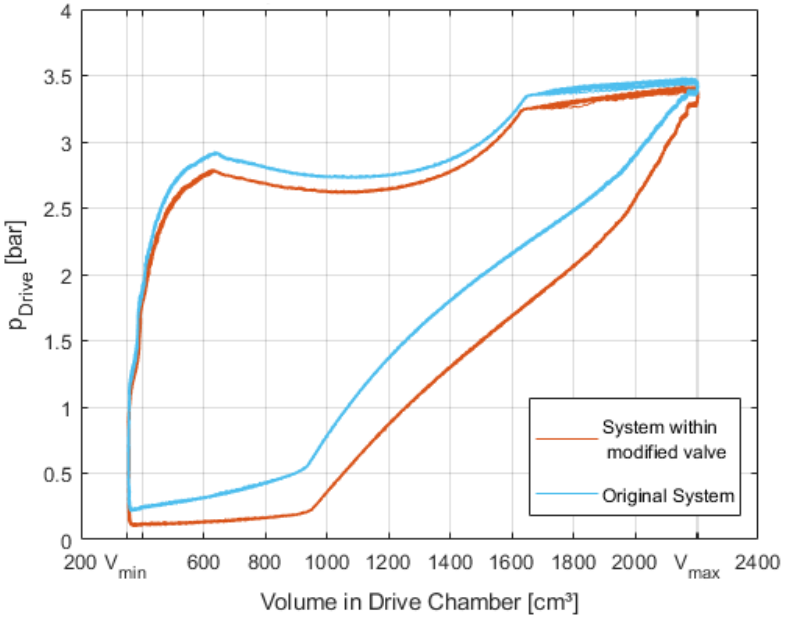

Figure 4.4: Measured pressure profile of drive chamber; effect of modification for upstream throttling

5. CONCLUSION AND OUTLOOK

5.1. Conclusion

Previous investigations in preparation for the measurements have shown that the usual throttling of the used pressure booster is unsuitable. A conversion to upstream throttling has been carried out. This has already shown an increase in performance. The simulative design of the spring was carried out using a grade 21 titanium alloy. Due to the availability on the market, a design was made for grade 5 titanium alloy and later on for stainless steel 1.4410. Due to the unfavourable stress position with a conical spring shape, the geometry was further developed in the direction of a rectangular plate. The resulting force curves were implemented in the simulation model. The results from this confirm the increase in efficiency due to the developed mechanics. The pressure level at the end of the stroke decreases as expected, which enables significant air savings. Due to the low-threshold load profiles of the springs, caused by the limitation of the stresses, several springs are required.

5.2. Outlook

To confirm the simulated results, measurements with the developed spring are pending. As soon as the current insufficient availability of titanium alloys, further simulations and measurements of the spring are necessary. The spring itself provides a corresponding maximum force depending on the preload. Since varying force levels are required depending on the supply pressure, the preload must be adapted to this. For initial tests, a mechanical

stressing mechanism via threaded rods is provided for this purpose. This tightens the clamping jaws and thus the edges of the spring. In the course of further work, this mechanism will be replaced by an adaptive alternative. A hydraulic system with transmission on the part of the supply pressure is conceivable here. This would make the system self-regulating. As soon as the test rig is available in its final configuration, the fatigue strength of the springs can be determined in order to assess the economic viability of the measure.

6. ACKNOWLEDGMENT

The research and development project Effipad - Efficient pneumatically driven pressure boosting - was funded by the European Union and the state of North Rhine-Westphalia. ifas would like to express its sincere thanks to all project partners, the European Regional Development Fund and the state of NRW.

7. NOMENCLATURE

$A_{P,D1}$	Area of piston in drive chamber (no. 1)
$A_{P,C1}$	Area of piston in compression chamber (no. 1)
b	Critical pressure ratio, 0.528
C	Sonic conductance
h	stroke
h_d	Stroke of dead volume
h_{max}	Maximal stroke
M_P	Mass of pistons including rod
p_C	Pressure in tank after compression
p_{Comp}	Pressure in compression chamber
$p_{D,passive}$	Pressure in Drive chamber during this is exhausted
$p_{s,D}$	Supply pressure for drive chamber
$p_{s,C}$	Supply pressure for compression chamber
R	Ideal gas constant
T	Temperature

8. REFERENCES

[1] K. Reddi, A. Elgowainy, N. Rustagi, E. Gupta, „Impact of hydrogen SAE J2601 fueling methods on fueling time of light duty fuel cell electric vehicles," Energy Systems Division, Argonne National Laboratory, South Cass Avenue, Argonne, 2017.

[2] F. Yang, K. Tadano, G. Li, T. Kagawa, „Analysis of the Energy Efficiency of a Pneumatic Booster Regulator with Energy Recovery," MDPI, Basel, August 2017.

[3] O. Reinertz, K. Schmitz, „Efficiency Optimized Pneumatic Pressure Booster," in *FPMC2019-1675, Symposium on Fluid Power and Motion Control*, Sarasota, October 2019.

[4] O. Reinertz, „Fluid-Driven Drive," WO, WO002020127886A1, 2020.

[5] O. Reinertz, K. Schmitz, „A Novel Exergy Efficient Pneumatic Vacuum Pump," in *FPMC2019-1675, 16. SICFP*, Tampere, Finland, May 2019.

[6] N.N., *Maximator Technical Data Sheet - Air Amplifier GPLV5, Release 03 / 2012 Page 1 of 3 • DB.01.02.01.04,* 2012.

[7] U. Risto, „Zur Charakterisierung und Anwendung des Durchschlagverhaltens von nachgiebigen rotationssymmetrischen Strukturen," Berichte der Illmenauer Mechanismentechnik (BIMT), TU Illmenau, Illmenau, October 2013.

[8] G. Arena, R. Groh, R. Theunissen, P. Weaver, A. Pirrera, „Adaptive Nonlinear Structures for Flow Regulation: Modelling Fluid-Structure Interactions with Coupled Eulerian-Lagrangian Meshes," in *SIMULIA UK Regional User Meeting*, 2016.

[9] L. Kashdan, C. Conner Seepersad, M. Haberman, P. Wilson, „Design, fabrication, and evaluation of negative stiffness elements using SLS," Mechanical Engineering Department and Applied Research Laboratory, University of Texas, Rapid Prototyping Journal, Austin, June 2011.

Biographies

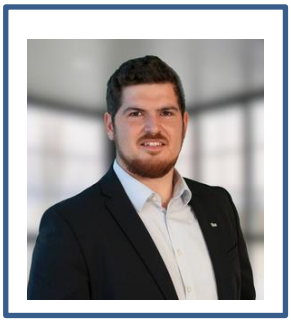

Matthias Schmid, received the bachelor's degree in mechanical engineering from Stuttgart University in 2016, the master's degree in mechanical engineering from Stuttgart University in 2020. He is currently working as a Research Associate at the Institute for Fluid Power Drives and Systems (ifas), RWTH Aachen University. His research areas include optimization of pneumatic systems focusing on energy efficiency and performance.

Olivier Reinertz received his diploma and his doctoral degree in mechanical engineering from RWTH Aachen University, Germany. He is currently Scientific Director at the Institute for Fluid Power Drives and Systems (ifas) at RWTH Aachen University. His research focuses on the model-based analysis of fluid power components and systems and the derivation and validation of innovative strategies for efficiency and performance optimization with an emphasis on compressed air and gas-powered systems.

Katharina Schmitz received a graduate's degree in mechanical engineering from RWTH Aachen University in 2010 and an engineering doctorate from RWTH Aachen University in 2015. She is currently the director of the Institute for Fluid Power Drives and Systems (ifas), RWTH Aachen University.